

# Combined Chemical and Thermal Sintering for High Conductivity Inkjet-printed Silver Nanoink on Flexible Substrates



This work is licensed under a Creative Commons Attribution 4.0 International License

I. Ivanišević, P. Kassal, A. Milinković, A. Rogina, and S. Milardović\*

Faculty of Chemical Engineering and Technology, University of Zagreb, Zagreb, Croatia

<https://doi.org/10.15255/CABEQ.2019.1585>

Original scientific paper  
Received: January 7, 2019  
Accepted: September 12, 2019

Electrical conductivity is a key factor in measuring performance of printed electronics, but the conductivity of inkjet-printed silver nanoinks greatly depends on post-fabrication sintering. In this work, two different conductive silver nanoinks, in which the silver nanoparticles were stabilized by two different capping agents – Poly(acrylic acid) (PAA) and Poly(methacrylic acid) (PMA) – were synthesized. The inks were inkjet-printed on flexible PET substrates, coated with an additional polycation layer, which facilitated chemical sintering. The printed features were then exposed to moderately elevated temperatures to evaluate the effect of combined chemical and thermal sintering. Both inks produced conductive features at room temperature, and the conductivity increased with both temperature and duration of sintering. At temperatures above 100 °C, the choice of capping agent had no pronounced effect on conductivity, which approached very high values of 50 % of bulk silver in all cases. The lowest resistivity (2.24  $\mu\Omega$  cm) was obtained after sintering at 120 °C for 180 min. By combining chemical and conventional thermal sintering, we have produced remarkably conductive silver electrodes on flexible substrates, while using low-cost and simple processes.

*Keywords:*

conductive ink, silver nanoparticles, inkjet printing, sintering, printed electronics

## Introduction

Owing to their superior optical and electrical characteristics, metal nanoparticles have become the focus of several fields of research, such as catalysis<sup>1,2</sup>, biomedicine and biosensors<sup>3,4</sup>, optics<sup>5</sup>, and electronics<sup>6,7</sup>. In the case of flexible electronics, inkjet printing of metal nanoparticle-based conductive inks has recently been utilized abundantly as an attractive technology to replace traditional electronics manufacturing processes<sup>7,8</sup>. Since it exhibits favorable properties in terms of electrical conductivity, stability against oxidation, and relatively low price for such properties, nanosilver is the material of choice for printed electronics<sup>7,9</sup>. The most utilized synthetic preparation routes of silver nanoparticles intended for conductive ink materials are chemical reduction with borohydride<sup>10</sup> and hydrazine<sup>11</sup>. Recently, numerous eco-friendly approaches have also been developed<sup>12–14</sup>.

Electrical conductivity is the crucial property of conductive inks for the mentioned applications. Therefore, obtaining the lowest possible resistance is the aim of most conductive ink formulations<sup>15</sup>. To

achieve lower resistivities, generally a sintering step is required after conductive ink deposition. The reason for this is the removal of the stabilizing agent coated around the metal nanoparticle, which forms an insulating shell after deposition. Capping (stabilizing) agents are essential for stability of colloidal silver solutions, used in printable conductive inks. Stabilizers can be various ionic species adsorbed on the nanocrystal surface, or polymer molecules that coat the nanocrystal surface to prevent the particles from precipitating<sup>16</sup>. To improve conductivity during sintering, the stabilizer needs to be removed, and this is usually achieved by exposing the printed features to elevated temperatures<sup>8,17</sup>. Typically, a temperature greater than 450 °C is required to obtain conductivities of 50 % of bulk silver or higher<sup>18,19</sup>. Kim *et al.* have thermally sintered their silver nanoparticle (AgNP) ink on different flexible polymeric substrates to obtain conductivities of around 50 % bulk Ag at temperatures above 200 °C<sup>20</sup>. However, common substrates for printed electronics are made of polymers that have low thermal stability and low glass transition temperatures<sup>7</sup>, and these elevated temperatures are considered too high.

Alternative sintering techniques have been studied and compared to thermal sintering<sup>7,21</sup>. For

\*Corresponding author: E-mail: [stjepan.milardovic@fkit.hr](mailto:stjepan.milardovic@fkit.hr)

example, photonic sintering uses broadband visible intense pulsed light to convert the metal precursor into its conductive counterparts<sup>22</sup>, and has been combined with microwave sintering to obtain highly conductive printed silver features<sup>23</sup>. Even higher conductivities (60 % of bulk Ag) were obtained by combining plasma and microwave sintering on polymer foils<sup>19</sup>. Electrical sintering, by applying a large voltage over the printed structure, which causes heating and sintering due to the induced current flow, has also yielded very conductive silver structures<sup>24</sup>. Recent utilization of ebeam technology for sintering has generated silver tracks with conductivities of approximately 36 % of bulk Ag<sup>25</sup>. In a direct comparison, however, it was found that plasma and laser sintering techniques generate lower conductivities than thermal sintering<sup>21</sup>.

A different sintering approach, one that eliminates the need for expensive instrumentation, is chemical sintering, which enables fabrication of conductive printed patterns at room temperature. In this approach, the stabilizer molecules on the AgNP surface are chemically desorbed or dissolved, thus causing the metal nanoparticles to come in contact with each other, forming a conductive path<sup>7,17</sup>. For example, chloride ions from different electrolytes can be used for chemical sintering: they remove the bulky stabilizer, such as Poly(acrylic acid) (PAA) or Polyvinylpyrrolidone (PVP), from the AgNP surface, which causes coalescence of the AgNPs<sup>26–28</sup>. HCl vapor has also been used for chemical sintering<sup>29</sup>, but conductivities of room temperature printed features have not surpassed 41 % of bulk silver<sup>26</sup>. Similarly, OH<sup>-</sup> ions can replace citrate stabilizers, and NaOH has also been used as a reagent for room-temperature sintering<sup>30</sup>. In one of the earliest instances of chemical sintering, Magdassi *et al.* have described the process of PAA stabilizer desorption by poly(diallyldimethylammonium chloride) (PDAC)<sup>31</sup>. After AgNP coalescence, these silver tracks exhibited conductivities of 20 % of bulk Ag. Similar conductivities were obtained by printing multiple layers of AgNP ink onto photo paper coated by a PDAC-like layer at room temperature<sup>32</sup>.

It is evident that most alternative sintering approaches cannot match conductivities obtained by thermal sintering. However, since high temperatures can be detrimental to the plastic substrates, we have tried to use combined chemical and thermal sintering at low–moderate temperatures to maximize printed silver conductivity. In this work, we have synthesized novel AgNP inks for inkjet printing, which contain Poly(acrylic acid) (PAA) or Poly(methacrylic acid) (PMA) as stabilizers. The conductive inks were deposited onto flexible PET substrates, pretreated with PDAC-like molecules for chemical sintering, after which they were thermally

sintered at different temperatures. This enabled evaluation of the combined effect of chemical and thermal sintering on the printed novel AgNP inks.

## Material and methods

### Materials and chemicals

Silver nitrate (AgNO<sub>3</sub>), as a metal precursor in all synthesis experiments, was obtained from VWR Chemicals (Belgium). Poly(acrylic acid) (PAA,  $M_w = 1800 \text{ g mol}^{-1}$ ), poly(methacrylic acid sodium salt) (PMA,  $M_w = 4000\text{--}6000 \text{ g mol}^{-1}$ ,  $w = 40 \%$  in water), ethylene glycol (EG; anhydrous,  $w = 99.8 \%$ ), hydrazine hydrate solution ( $w = 50\text{--}60 \%$ ), and 2-amino-2-methyl-1-propanol (2-AMP) were purchased from Sigma-Aldrich (USA). Citric acid and sodium hydroxide (NaOH) were purchased from Gram Mol (Croatia), Kemika (Croatia), respectively. All applied chemicals were of analytical grade and used as received. Deionized water, purified using a Millipore-MilliQ system, was used in all syntheses. The precoated flexible PET substrate (Nov-ele™) for inkjet printing was obtained from Novacentrix (USA).

### Synthesis and characterization of silver nanoparticle-based conductive ink

The wet chemistry synthesis of silver nanoparticles was based on our previous work<sup>33</sup>, with some modifications. In this work, 20 mL of a 1.15 mol dm<sup>-3</sup> NaOH solution was first mixed with an equimolar solution of silver nitrate. After washing the silver oxide precipitate, the capping agent – either PAA or PMA – was added to the reaction mixture. Reduction was carried out with hydrazine solution, which was accurately added using a Gilson Miniplus Evolution peristaltic pump fitted with a MF4 pump head (France). The polyacid stabilized silver nanoparticles (PAA-Ag or PMA-Ag) were then agglomerated by adding 0.1 mol dm<sup>-3</sup> citric acid. The precipitated nanosilver was washed with water and acetone, after which the wet sediment was dried at 60 °C. The conductive ink was made by mixing the dried PAA-AgNPs or PMA-AgNPs into an EG solution (mass fraction,  $w = 20 \%$ ). A small amount of 2-AMP was added for adjusting the pH value to 10.5. Homogenization of the prepared conductive inks was performed using Bاندelin electronic Sonorex high-power ultrasound bath (Germany) and Stuart SA8 vortex mixer (UK). The particle size distribution analysis (Dynamic light scattering method, DLS), as well as the electrokinetic potential measurements of the coated silver NPs, were performed using a ZetaPlus (Brookhaven Instruments Corporation, USA) instrument.

## Inkjet printing and sintering

The PAA-AgNP and PMA-AgNP-based conductive inks were loaded into the cartridges of the inkjet printer (modified flatbed Epson Stylus D92) and deposited onto flexible substrates to form conductive patterns. The used printer had a maximum resolution of 5760 x 1440 dpi and 90 nozzles for black ink, and 29 nozzles for each of the three colors: cyan, magenta, and yellow. Prior to printing, all four corresponding cartridges were loaded with 5 mL of the conductive ink using a pipette. The features for printing were designed in CorelDraw X8 software. In the Epson printing settings, the quality was set to “Best photo”, the paper setting to “Epson matte”, the “Photo enhance” setting was selected, and the “High speed” printing option was disabled. The commercial flexible PET substrates were already coated with an adhesion layer, enabling chemical sintering at room temperature. The printed flexible conductive features were additionally thermally sintered in an oven for 20 min at temperatures ranging from 60 to 140 °C.

In the next set of experiments, the flexible conductive features were sintered at 120 °C for different durations: from 30 to 180 min.

The surface morphology and thickness ( $n = 5$ ) of the printed silver lines were imaged by a scanning electron microscope (Tescan Vega 3 SEM Easyprobe, Czech Republic) at electron beam energy of 10 keV. For thickness measurements, the devices were cut by scalpel and thickness of the cross-section was determined in five independent parts of the line. A digital multimeter 34461A, 6 ½ Digit, Truevolt DMM, Keysight (USA) with an in-line four-point probe was used for resistance measurements. Four-point measurements were used in order to account for contact resistances<sup>34</sup>. Resistivity of printed patterns was calculated from the printed line resistance ( $R$ ), measured by the digital multimeter with four-point probe, and the thickness profile ( $h$ ), the average value obtained by SEM imaging, according to the equation:  $\rho = Rwh/l$ , where  $w$  and  $l$  are the line width and length, respectively<sup>15</sup>.

## Results and discussion

### Silver nanoparticle-based conductive ink

While developing metal nanoparticle-based inks for inkjet printing, several parameters must be taken into account to avoid problems with printer performance. A major problem that can affect the inkjet printing process is nozzle clogging. Clogging can occur if the particles are relatively large (larger than 50 nm), or if they tend to agglomerate<sup>35</sup>. Hence, the nanoparticle size and colloid stability need to be

carefully monitored during conductive ink synthesis.

We have recently reported on the synthesis of AgNP ink suitable for inkjet printing, which contained PAA as the capping agent<sup>33</sup>. Here, we expanded on this research by additionally evaluating PMA as capping agent and studying the effect of thermal sintering on conductivity of both inks. Both Poly(acrylic acid) and Poly(methacrylic acid) can be used as stabilizing agents of metal nanoparticles due to the existence of carboxylic groups<sup>36</sup>. In basic media, both polyacids are deprotonated, the nanograins have a negative surface charge, and suspensions are thus electrostatically stabilized. The electrokinetic potential (Zeta potential) gives the tendency of particles to agglomerate or to sediment, and is a measure of colloid stability. The zeta potential values for inks based on PAA-AgNP and PMA-AgNP were found to be  $-46.92 \pm 0.83$  mV and  $-35.49 \pm 1.48$  mV, respectively. These values indicate that both suspensions are stable and can be used for inkjet printing.

With nanoparticle size being another crucial parameter in inkjet ink formulations, we investigated particle size by DLS, Fig. 1. The average diameter of PAA-AgNPs was  $1.90 \pm 0.04$  nm, while PMA-AgNPs were larger, with an average diameter of  $18.10 \pm 0.18$  nm. Both types of AgNPs were relatively small compared to spherical silver nanoparticles for inkjet printing found in the literature, which range in size from 10 to 80 nm<sup>17</sup>. A narrow size distribution was achieved in both cases.

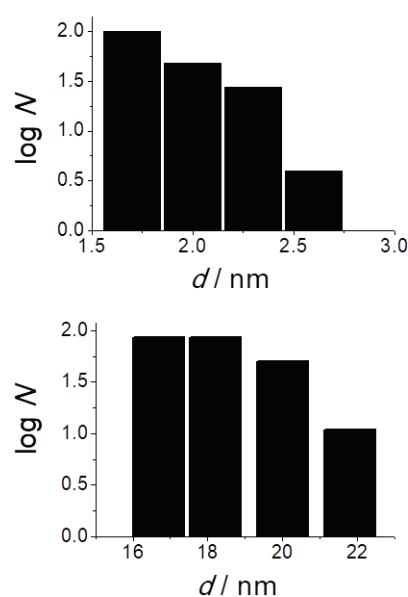


Fig. 1 – Particle size distribution of PAA-stabilized AgNPs (top) and PMA-stabilized AgNPs (bottom). Sample dilution was in all cases  $\phi = 1:30000$ .

The small particle size and highly negative zeta potential indicated that the inks were suitable for inkjet printing, with no potential danger of printer nozzle clogging. After characterization, both PAA-AgNP and PMA-AgNP inks were deposited by an inkjet printer onto flexible PET substrates (Fig. 2), after which the effect of thermal sintering was studied.

### Effect of chemical and thermal sintering on resistivity

Due to the PDAC-like coating on the flexible PET foils, which caused a chemical sintering process, the printed silver electrodes were conductive even after drying at room temperature. The resistivities at room temperature (without thermal sintering) were  $35.7 \mu\Omega \text{ cm}$  for PAA-AgNP electrodes, and  $13.7 \mu\Omega \text{ cm}$  for PMA-AgNP electrodes, which corresponded to 4.45 % and 11.6 % conductivity of bulk silver, respectively. These room temperature conductivities have already been explained: the positively charged polymer in the adhesion layer of the commercial PET films causes desorption of the negatively charged PAA and PMA from the nanoparticle surface, which leaves the particles without their stabilizer and causes their coalescence, thus improving conductivity<sup>31,37</sup>. SEM images confirm that a relatively homogeneous conductive silver layer was obtained even at room temperature (Fig. 3a). The observed room-temperature conductivities were generally close to those for chemically sintered AgNPs found in the literature<sup>30,38,39</sup>.

Upon exposure of the printed silver electrodes to elevated temperatures for 20 min, the resistivity decreased (Fig. 4). We could notice that the initial decrease in resistivity of the PAA-AgNP electrodes was more pronounced than of PMA-AgNP electrodes. The PAA-AgNP particles are smaller, hence a greater degree of sintering can be achieved at lower temperatures<sup>20</sup>. However, this effect becomes negligible at elevated temperatures (i.e., higher degrees of sintering), which has also been previously observed<sup>20</sup>. In both cases, the minimum resistivity after 20 min was achieved at the highest temperature. This was in the case of PAA-AgNP electrodes  $3.26 \mu\Omega \text{ cm}$  (49 % conductivity of bulk Ag), and in the case of PMA-AgNP electrodes  $3.11 \mu\Omega \text{ cm}$  (51 % conductivity of bulk Ag). The highly conductive homogeneous silver layer obtained at  $140 \text{ }^\circ\text{C}$  was confirmed by SEM imaging (Fig. 3b). At temperatures greater than  $100 \text{ }^\circ\text{C}$ , both inks produced similar resistivities of about  $3.3 \pm 0.2 \mu\Omega \text{ cm}$ , which is a conductivity of around 48 % of bulk silver. However, deformation (i.e., bending) of the PET substrates was noticed at the highest temperature. This suggests that lower temperatures, of about  $100 \text{ }^\circ\text{C} - 120 \text{ }^\circ\text{C}$ , can be used for thermal sintering,

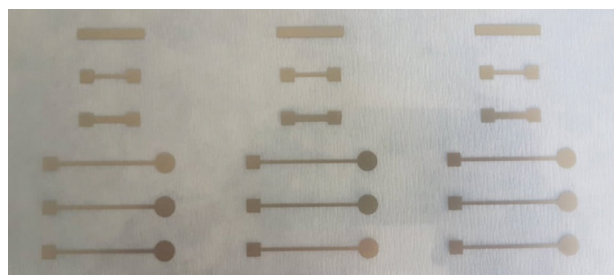


Fig. 2 – Inkjet-printed silver features on flexible PET films. From top to bottom: lines for SEM imaging and thickness calculation, lines for resistance measurement, planar electrodes for potential electrochemical measurements (not included in this study).

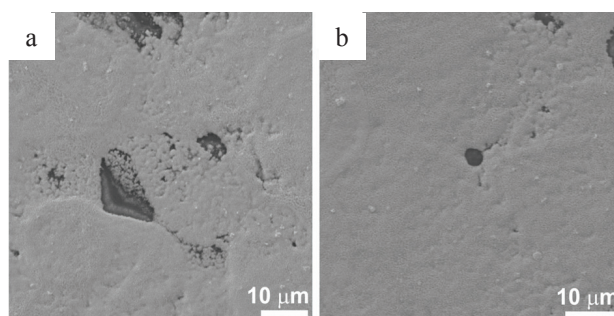


Fig. 3 – SEM image of PAA-AgNP surface after sintering a) at room temperature; and b) at  $140 \text{ }^\circ\text{C}$  for 20 min

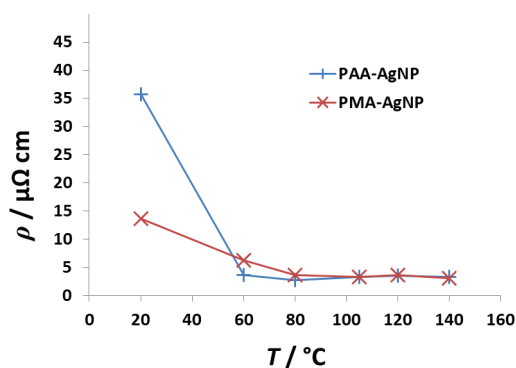


Fig. 4 – Change in electrical resistivity of PAA-AgNP and PMA-AgNP printed silver features, after thermal sintering at different temperatures for 20 min

with no significantly detrimental effect to the printed silver conductivity.

The effect of thermal sintering at  $120 \text{ }^\circ\text{C}$  for periods up to 180 min was evaluated next. In the case of silver tracks based on PAA-AgNP ink, sintering for different durations had no pronounced effect on conductivity. All PAA-AgNP silver tracks exhibited very low resistivities of  $2.1 - 3.1 \mu\Omega \text{ cm}$ , with no apparent trend. In the case of PMA-AgNP ink, heating at  $120 \text{ }^\circ\text{C}$  for prolonged duration caused a very gradual decrease in resistivity, reaching a minimum value of  $2.24 \mu\Omega \text{ cm}$  (71 % of bulk Ag conductivity) after 180 min. This was confirmed by

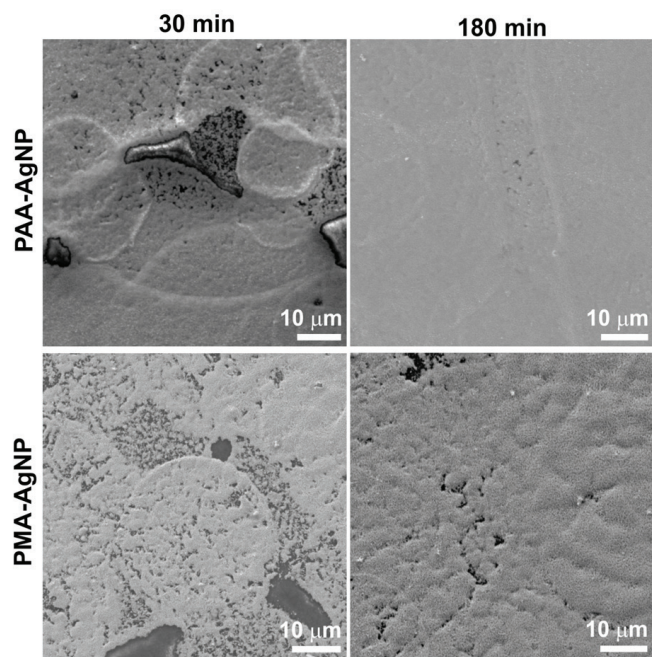


Fig. 5 – SEM images of printed surface of PAA-AgNP and PMA-AgNP ink after sintering at 120 °C for different sintering times (30 and 180 min)

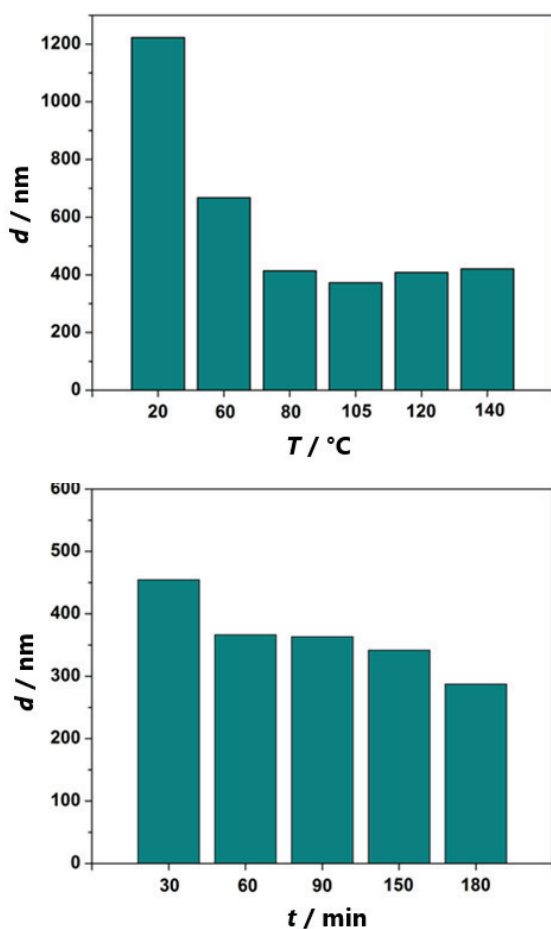


Fig. 6 – Thickness of PMA-AgNP printed layers sintered at different temperatures for 20 min and for different durations at 120 °C, obtained by scanning electron microscopy of cross-section

SEM imaging (Fig. 5), where it was visible that a remarkably high degree of sintering had been achieved after 180 min, both with PAA-AgNP and PMA-AgNP inks. These exceptionally high conductivities confirm the effectiveness of the combination chemical/thermal sintering process for our AgNP inks. For comparison, previous additional thermal sintering of PDAC sintered silver patterns yielded conductivities up to 40 % of bulk Ag<sup>32</sup>.

Thermal sintering generally has the same effect on printed layer thickness ( $h$ ) as it does on resistivity. That is, the thickness of the printed silver layer decreases with both increasing temperature and sintering time (Fig. 6). This can be attributed to a loss of stabilizer molecules during heating, which in turn enables formation of more compact, thinner layers. For example, a clear difference in the printed layer thickness can be seen from a cross-sectional SEM image of printed PMA-AgNP ink, between samples sintered at room temperature and at 105 °C for 20 min, Fig. 7.

#### Effect of sintering on printed line width

Minimum conductive line width is generally a function of printer resolution and printing settings. However, sintering causes critical changes in morphology of a printed layer and facilitates formation of continuous interconnects between silver nanoparticles<sup>8</sup>. We therefore evaluated the effect of sintering at a moderate temperature on line width, by measuring resistances of different widths of printed silver lines, Fig. 8a. The resistances of three different sets of PMA-AgNP lines, measured after sintering for 30 min at 105 °C, are given in Table 1. The evaluated width was from 30 μm to 2 mm. The minimum line width that was conductive in all cases was 200 μm. This was also confirmed by optical microscopy (Fig. 8b), where it was visible that a conductive path had not formed below a width of 200 μm. A large variability in the measured resistances was apparent for minimum conductive line widths (200 μm and 300 μm).

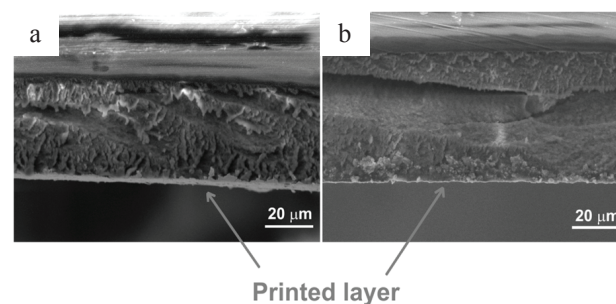


Fig. 7 – Cross-sectional SEM image of printed PMA-AgNP silver layers after sintering a) at room temperature; and b) at 105 °C for 20 minutes

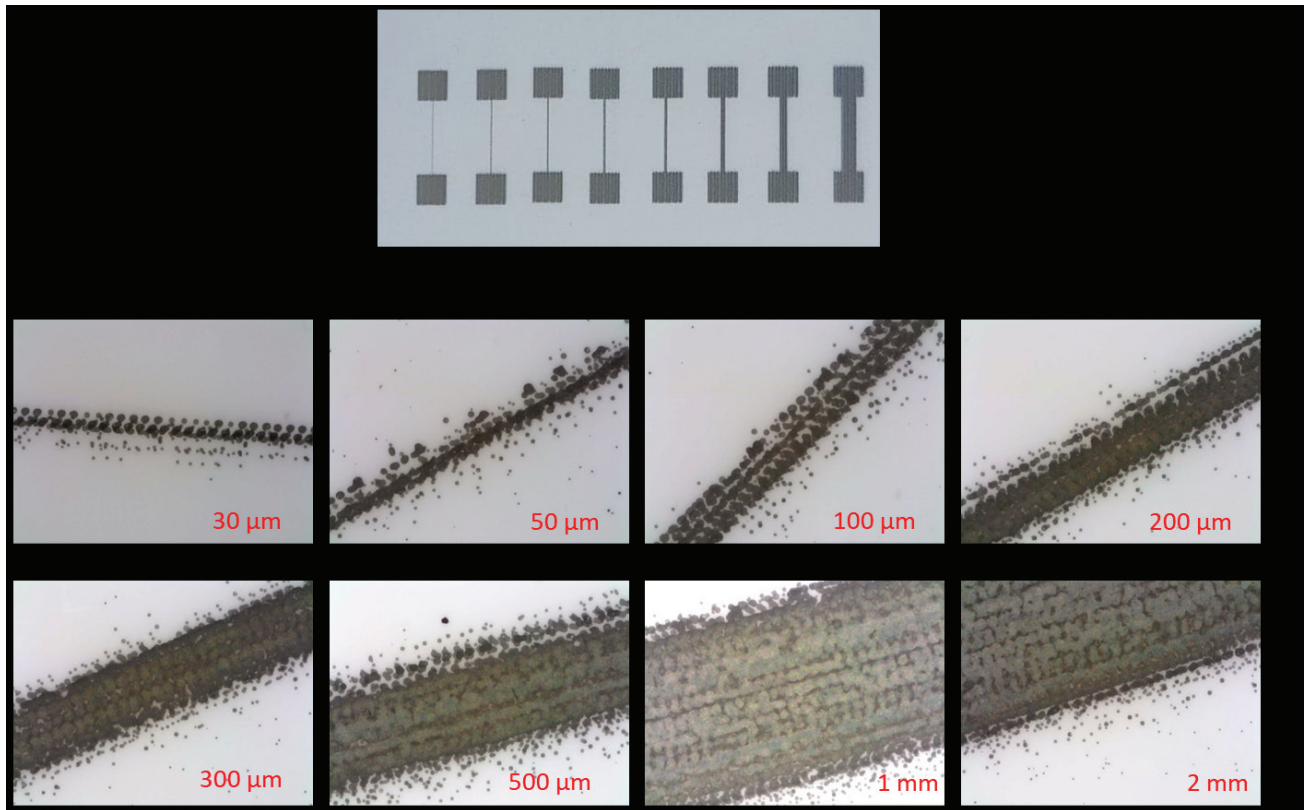


Fig. 8 – a) Printed PMA-AgNP silver lines of different widths; and b) corresponding optical microscopy images (Magnification: 200 $\times$ )

Table 1 – Resistances of three sets of printed PMA-AgNP lines with varying widths ( $w$ ), measured after sintering at 105 °C for 30 min

$w / \text{mm}$	$R / \Omega$		
	1. set	2. set	3. set
0.03	×	×	×
0.05	297.7	×	×
0.10	×	×	175.9
0.20	37.5	48.4	77.4
0.30	20.3	25.1	23.6
0.50	10.7	11.5	11.1
1.00	5.3	4.6	5.2
2.00	2.8	2.4	2.8

## Conclusions

We have developed two conductive silver nanoparticle-based inks using Poly(acrylic acid) and Poly(methacrylic acid) as stabilizers. Both inks were suitable for inkjet printing, and the printed features were conductive at room temperature due

to the chemical sintering effect, with PMA-AgNP exhibiting a somewhat greater conductivity. The conductivity was further improved by thermal sintering at elevated temperatures. At temperatures above 100 °C, the choice of polymer stabilizer had no pronounced effect on conductivity, which approached very high values of 50 % of bulk silver in all cases. Thermal sintering at a moderate temperature (120 °C) over extended time periods generated silver lines with exceptionally high values of conductivity (71 % of bulk Ag). A minimum conductive line width was determined to be 200 μm after sintering at 105 °C for 30 min. Although implementation of thermal sintering in the mass production of plastic electronics presents a challenge, this approach can readily be adapted to sintering of smaller batches. We have demonstrated outstanding conductivities of inkjet-printed flexible silver electrodes, which cannot easily be met by using alternative sintering methods.

## ACKNOWLEDGEMENTS

The authors are grateful to the University of Zagreb (Grant No. 118020) for financial support. Special thanks to Prof. Tajana Preočanin from the Faculty of Science, University of Zagreb, for use of the Zetaplus instrument.

## References

1. *Viswanathan, P., Ramaraj, R.*, Preparation of polyelectrolyte-stabilized silver nanoparticles for catalytic applications, *Polym. Int.* **66** (2017) 342.  
doi: <https://doi.org/10.1002/pi.5178>
2. *Kosevic, M. G., Sekularac, G. M., Panic, V. V.*, On the stability of platinum-composite electrocatalysts prepared with different substrate materials, *J. Electrochem. Sci. Eng.* **6** (2016) 29.  
doi: <https://doi.org/10.1002/10.5599/jese.269>
3. *Cohen-Karni, T., Langer, R., Kohane, D. S.*, The smartest materials: The future of nanoelectronics in medicine, *ACS Nano* **6** (2012) 6541.  
doi: <https://doi.org/10.1021/nn302915s>
4. *Maduraiveeran, G., Sasidharan, M., Ganesan, V.*, Electrochemical sensor and biosensor platforms based on advanced nanomaterials for biological and biomedical applications, *Biosens. Bioelectron.* **103** (2018) 113.  
doi: <https://doi.org/10.1016/j.bios.2017.12.031>
5. *Fratoddi, I.*, Hydrophobic and hydrophilic Au and Ag nanoparticles. Breakthroughs and perspectives, *Nanomaterials* **8** (2018) 25.  
doi: <https://doi.org/10.3390/nano8010011>
6. *Lu, W., Lieber, C. M.*, Nanoelectronics from the bottom up, *Nat. Mater.* **6** (2007) 841.  
doi: <https://doi.org/10.1038/nmat2028>
7. *Wunscher, S., Abbel, R., Perelaer, J., Schubert, U. S.*, Progress of alternative sintering approaches of inkjet-printed metal inks and their application for manufacturing of flexible electronic devices, *J. Mater. Chem. C* **2** (2014) 10232.  
doi: <https://doi.org/10.1039/c4tc01820f>
8. *Kamyshny, A., Magdassi, S.*, Conductive nanomaterials for printed electronics, *Small* **10** (2014) 3515.  
doi: <https://doi.org/10.1002/sml.201303000>
9. *Ghorbani, H. R., Safekordi, A. A., Attar, H., Sorkhabadi, S. M. R.*, Biological and non-biological methods for silver nanoparticles synthesis, *Chem. Biochem. Eng. Q.* **25** (2011) 317.
10. *Mendis, P., de Silva, R. M., de Silva, K. M. N., Wijenayaka, L. A., Jayawardana, K., Yan, M.*, Nanosilver rainbow: A rapid and facile method to tune different colours of nanosilver through the controlled synthesis of stable spherical silver nanoparticles, *RSC Adv.* **6** (2016) 48792.  
doi: <https://doi.org/10.1039/c6ra08336f>
11. *Ivanišević, I., Rukavina, V., Kassal, P., Milardović, S.*, Impact of weak organic acids on precipitation of poly(acrylic acid) stabilized silver nanoparticles; an electrochemical approach, *Croat. Chem. Acta* **91** (2019) 491.  
doi: <https://doi.org/10.5562/cca3445>
12. *Jorge de Souza, T. A., Rosa Souza, L. R., Franchi, L. P.*, Silver nanoparticles: An integrated view of green synthesis methods, transformation in the environment, and toxicity, *Ecotoxicol. Environ. Saf.* **171** (2019) 691.  
doi: <https://doi.org/10.1016/j.ecoenv.2018.12.095>
13. *Said, M. I., Othman, A. A.*, Fast green synthesis of silver nanoparticles using grape leaves extract, *Mater. Res. Express* **6** (2019).  
doi: <https://doi.org/10.1088/2053-1591/ab0481>
14. *Behravan, M., Panahi, A. H., Naghizadeh, A., Ziaee, M., Mandavi, R., Mirzapour, A.*, Facile green synthesis of silver nanoparticles using *Berberis vulgaris* leaf and root aqueous extract and its antibacterial activity, *Int. J. Biol. Macromol.* **124** (2019) 148.  
doi: <https://doi.org/10.1016/j.ijbiomac.2018.11.101>
15. *Nir, M. M., Zamir, D., Haymov, I., Ben-Asher, L., Cohen, O., Faulkner, B., Vega, F. d. l.*, Electrically Conductive Inks for Inkjet Printing, in Magdassi, S. (Editor), *The Chemistry of Inkjet Inks*, World Scientific Publishing, Singapore, 2010, pp 225–254.  
doi: [https://doi.org/10.1142/9789812818225\\_0012](https://doi.org/10.1142/9789812818225_0012)
16. *Li, C. C., Chang, S. J., Su, F. J., Lin, S. W., Chou, Y. C.*, Effects of capping agents on the dispersion of silver nanoparticles, *Colloid Surf. A-Physicochem. Eng. Asp.* **419** (2013) 209.  
doi: <https://doi.org/10.1016/j.colsurfa.2012.11.077>
17. *Zhu, D. B., Wu, M. Q.*, Highly conductive nano-silver circuits by inkjet printing, *J. Electron. Mater.* **47** (2018) 5133.  
doi: <https://doi.org/10.1007/s11664-018-6418-z>
18. *Perelaer, J., de Laat, A. W. M., Hendriks, C. E., Schubert, U. S.*, Inkjet-printed silver tracks: Low temperature curing and thermal stability investigation, *J. Mater. Chem.* **18** (2008) 3209.  
doi: <https://doi.org/10.1039/b720032c>
19. *Perelaer, J., Jani, R., Grouchko, M., Kamyshny, A., Magdassi, S., Schubert, U. S.*, Plasma and microwave flash sintering of a tailored silver nanoparticle ink, yielding 60 % bulk conductivity on cost-effective polymer foils, *Adv. Mater.* **24** (2012) 3993.  
doi: <https://doi.org/10.1002/adma.201200899>
20. *Kim, D., Moon, J.*, Highly conductive ink jet printed films of nanosilver particles for printable electronics, *Electrochem. Solid State Lett.* **8** (2005) J30.  
doi: <https://doi.org/10.1149/1.2073670>
21. *Niittynen, J., Abbel, R., Mantysalo, M., Perelaer, J., Schubert, U. S., Lupo, D.*, Alternative sintering methods compared to conventional thermal sintering for inkjet printed silver nanoparticle ink, *Thin Solid Films* **556** (2014) 452.  
doi: <https://doi.org/10.1016/j.tsf.2014.02.001>
22. *Kim, H. S., Dhage, S. R., Shim, D. E., Hahn, H. T.*, Intense pulsed light sintering of copper nanoink for printed electronics, *Appl. Phys. A: Mater. Sci. Process.* **97** (2009) 791.  
doi: <https://doi.org/10.1007/s00339-009-5360-6>
23. *Perelaer, J., Abbel, R., Wunscher, S., Jani, R., van Lammeren, T., Schubert, U. S.*, Roll-to-roll compatible sintering of inkjet printed features by photonic and microwave exposure: From non-conductive ink to 40 % bulk silver conductivity in less than 15 seconds, *Adv. Mater.* **24** (2012) 2620.  
doi: <https://doi.org/10.1002/adma.201104417>
24. *Allen, M. L., Aronniemi, M., Mattila, T., Alastalo, A., Ojanpera, K., Suhonen, M., Seppa, H.*, Electrical sintering of nanoparticle structures, *Nanotechnology* **19** (2008) 175201.  
doi: <https://doi.org/10.1088/0957-4484/19/17/175201>
25. *Farrar, Y., Biemann, M., Magdassi, S.*, Inkjet printing and rapid ebeam sintering enable formation of highly conductive patterns in roll to roll process, *RSC Adv.* **7** (2017) 15463.  
doi: <https://doi.org/10.1039/c7ra00967d>
26. *Grouchko, M., Kamyshny, A., Mihailescu, C. F., Anghel, D. F., Magdassi, S.*, Conductive inks with a “built-in” mechanism that enables sintering at room temperature, *ACS Nano* **5** (2011) 3354.  
doi: <https://doi.org/10.1021/nn2005848>
27. *Hui, Z., Liu, Y. G., Guo, W., Li, L. H., Mu, N., Jin, C., Zhu, Y., Peng, P.*, Chemical sintering of direct-written silver nanowire flexible electrodes under room temperature, *Nanotechnology* **28** (2017) 285703.  
doi: <https://doi.org/10.1088/1361-6528/aa76ce>

28. Tang, Y., He, W., Wang, S. X., Tao, Z. H., Cheng, L. J., New insight into the size-controlled synthesis of silver nanoparticles and its superiority in room temperature sintering, *CrystEngComm*. **16** (2014) 4431.  
doi: <https://doi.org/10.1039/c3ce42439a>
29. Shi, L. B., Layani, M., Cai, X., Zhao, H. L., Magdassi, S., Lan, M. B., An inkjet printed Ag electrode fabricated on plastic substrate with a chemical sintering approach for the electrochemical sensing of hydrogen peroxide, *Sensors. Actuators, B* **256** (2018) 938.  
doi: <https://doi.org/10.1016/j.snb.2017.10.035>
30. Xiao, Y., Zhang, Z. H., Yang, M., Yang, H. F., Li, M. Y., Cao, Y., The effect of NaOH on room-temperature sintering of Ag nanoparticles for high-performance flexible electronic application, *Mater. Lett.* **222** (2018) 16.  
doi: <https://doi.org/10.1016/j.matlet.2018.03.164>
31. Magdassi, S., Grouchko, M., Berezin, O., Kamysny, A., Triggering the sintering of silver nanoparticles at room temperature, *ACS Nano* **4** (2010) 1943.  
doi: <https://doi.org/10.1021/nn901868t>
32. Shen, W. F., Zhang, X. P., Huang, Q. J., Xu, Q. S., Song, W. J., Preparation of solid silver nanoparticles for inkjet printed flexible electronics with high conductivity, *Nanoscale* **6** (2014) 1622.  
doi: <https://doi.org/10.1039/c3nr05479a>
33. Milardović, S., Ivanišević, I., Rogina, A., Kassal, P., Synthesis and electrochemical characterization of AgNP ink suitable for inkjet printing, *Int. J. Electrochem. Sci.* **13** (2018) 11136.  
doi: <https://doi.org/10.20964/2018.11.87>
34. Heaney, M. B., Electrical Conductivity and Resistivity, in Webster, J.G. (Editor), *Measurement, Instrumentation, and Sensors Handbook*, CRC Press LLC, Boca Raton, 1999, pp 1308–1321.  
doi: <https://doi.org/10.1201/b15664-29>
35. Dang, M. C., Dang, T. M. D., Fribourg-Blanc, E., Silver nanoparticles ink synthesis for conductive patterns fabrication using inkjet printing technology, *Adv. Nat. Sci.-Nanosci. Nanotechnol.* **6** (2015) 8.  
doi: <https://doi.org/10.1088/2043-6262/6/1/015003>
36. Huang, Q. J., Shen, W. F., Xu, Q. S., Tan, R. Q., Song, W. J., Properties of polyacrylic acid-coated silver nanoparticle ink for inkjet printing conductive tracks on paper with high conductivity, *Mater. Chem. Phys.* **147** (2014) 550.  
doi: <https://doi.org/10.1016/j.matchemphys.2014.05.030>
37. Rojas, O. J., Ernstsson, M., Neuman, R. D., Claesson, P. M., Effect of polyelectrolyte charge density on the adsorption and desorption behavior on mica, *Langmuir* **18** (2002) 1604.  
doi: <https://doi.org/10.1021/la0155698>
38. Lee, M. Y., Lee, W. J., Roy, A. K., Lee, K. S., Park, S. Y., Lee, J. H., In, I., Room-temperature sinterable silver nanoparticle ink with low-molecular-weight poly(N-vinylpyrrolidone) ligand, *Chem. Lett.* **42** (2013) 232.  
doi: <https://doi.org/10.1246/cl.2013.232>
39. Zhang, X. Y., Xu, J. J., Wu, J. Y., Shan, F., Ma, X. D., Chen, Y. Z., Zhang, T., Seeds triggered massive synthesis and multi-step room temperature post-processing of silver nanoink-application for paper electronics, *RSC Adv.* **7** (2017) 8.  
doi: <https://doi.org/10.1039/c6ra27163d>